

Analysis and Control of Three-Phase Interleaved SCC-LLC Resonant Converter Load Sharing Considering Component Tolerance

Bo Sheng, Xiang Zhou, Wenbo Liu, Yang Chen, Yan-Fei Liu, *Fellow, IEEE*, Paresh C. Sen, *Life Fellow IEEE*

Department of Electrical and Computer Engineering

Queen's University,
Kingston, Canada

bo.sheng@queensu.ca, yanfei.liu@queensu.ca

Abstract—The conduction loss becomes extremely large if applied LLC converter in high power electrical vehicle (EV) applications. Interleaving technique can help reduce the conduction loss and expand load capacity for LLC converter. However, component tolerance on resonant tanks causes load sharing problem, leading to severe performance degrading. To solve the problem, Switch-controlled Capacitor (SCC) circuit is added into resonant tanks to offset the component tolerance through reducing equivalent resonant capacitance. The load sharing characteristic of a three-phase LLC converter with and without SCC circuit is analyzed. The proposed control strategy reduces the SCC MOSFET voltage stress. Thus, lower voltage rating MOSFET which usually features of lower turn-on resistance can be used. Phase shedding technique is also performed to improve the light load efficiency. A prototype of a 250V – 430V input, 14V/260A output three-phase SCC-LLC prototype has been built and tested. Experimental results demonstrate the effectiveness of the SCC circuit and the proposed control strategy. Good current sharing performance among three phases is obtained. In addition, a peak efficiency of 96.7% and a full load efficiency of 95.8% are achieved at 380V input.

Keywords – LLC resonant converter, switch-controlled capacitor, current sharing, digital comparison control strategy

I. INTRODUCTION

Along with the development of the electric vehicles (EVs), more and more auxiliary equipment is added to improve consumer experience. The EV power train system consists of high voltage (HV) Li-Ion batteries (200V~450V), low voltage (LV) Lead-acid batteries (9V~16V), and the DC/DC converters as shown in Fig. 1.

In general, HV batteries provide power for traction motor drives. On the other hand, LV batteries provide power for auxiliary devices including lighting, audio/video systems, air conditioners, automatic seats, and etc. The HV battery is usually charged from the grid via on-board or off-board chargers. The LV battery is usually charged by the HV battery through an isolated high step-down DC/DC converter (450V to 9V) [1]. Of all resonant converters, LLC configuration provides many added benefits over other resonant configurations. It could not only achieve zero

voltage switching (ZVS) for primary side switches, but zero current switching (ZCS) for secondary side switches. The LLC converter has been widely accepted in recent years by providing both high efficiency and high power density, which makes it an excellent candidate for the HV to LV DC/DC converter [2, 3].

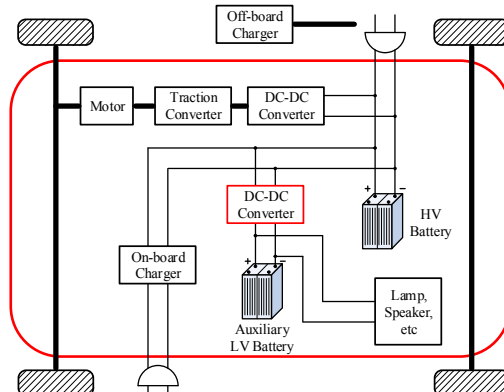


Fig. 1. Diagram of the EV power train

The power rating of EV auxiliary devices is at least 2.5kW. Therefore, LLC converter needs to provide more than 200A load at 9V~16V output voltage. With such high current, the converter will experience several limitations, including, 1) high conduction loss; 2) high current stress; 3) high voltage and current ripple. Particularly, high conduction loss results in poor thermal performance or even worse breakdown of the system. Interleaving technique has been verified to solve the limitations and expand the load capacity for LLC converter. However, when interleaved, all phases have to operate at same switching frequency. If taking resonant tank components tolerance into consideration, the voltage gain of each phase at same switching frequency is different from each other. This difference will cause extremely output current unbalance and efficiency degrading.

The concept of Switch-controlled capacitor (SCC) was introduced in [4]. It could help modify the voltage gain through reducing equivalent resonant capacitance. Both half-wave SCC and full-wave SCC have been successfully

applied into two-phase LLC resonant converter to achieve interleaving and load sharing [5, 6]. The authors either combined fixed switching frequency with full-wave SCC or variable switching frequency with half-wave SCC.

In this paper, full-wave SCC is applied on each phase in a three-phase LLC EV charger. The topology of three-phase interleaved full-wave SCC-LLC converter is shown in Fig. 2. The SCC MOSFETs along with the capacitor C_a and C_s together form the equivalent resonant capacitor. Ideally, the 260A full load will be equally distributed into three phases. Thus, each phase only needs to be designed to carry 90A current. Due to the existing of the full-wave SCC

on every phase, current sharing could be achieved no matter which phase carries the highest or the lowest current. A digital comparison control scheme is proposed to control the SCC MOSFETs. The proposed control strategy is implemented into a micro-controller unit (MCU).

This paper is organized as follows. Section II introduces the operation principle of a full-wave SCC. Section III analyzes the load sharing characteristic of three-phase LLC converter with and without SCC. Section IV explains the details of the proposed digital comparison control strategy. Experimental results and a conclusion are provided in Section V and Section VI, respectively.

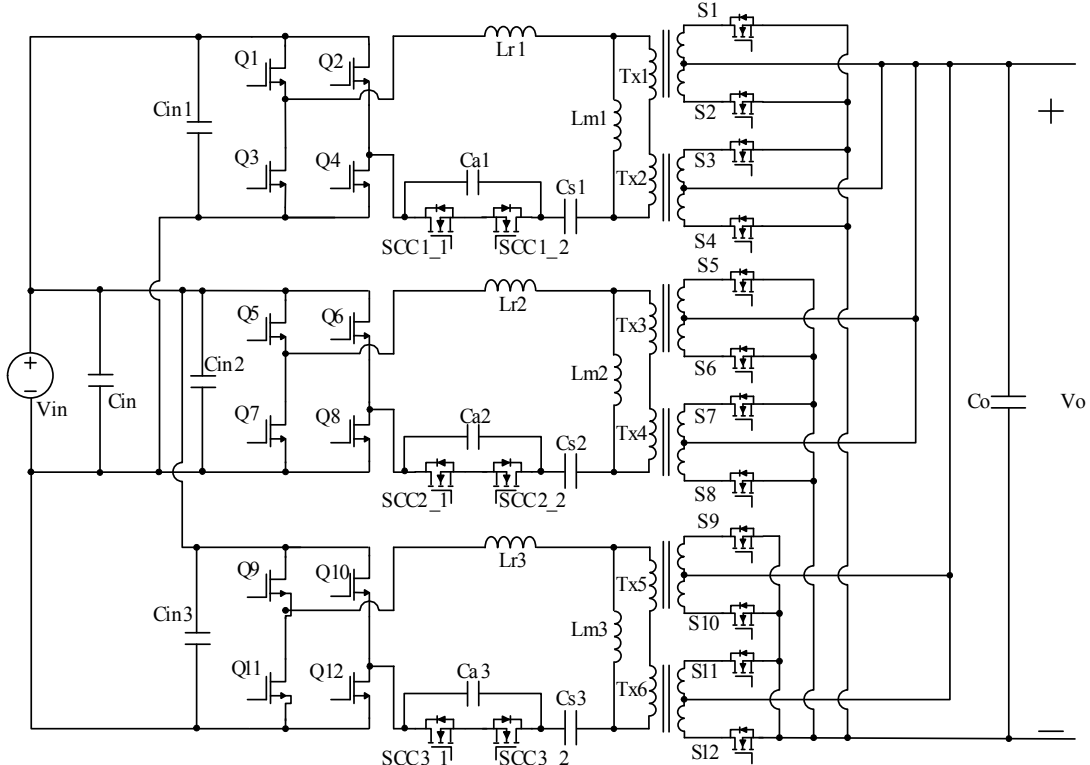


Fig. 2. Topology of three-phase interleaved SCC-LLC resonant converter

II. OPERATION PRINCIPLE OF FULL-WAVE SCC CIRCUIT

The structure of a full-wave SCC circuit is shown in Fig. 3. The circuit consists a capacitor in parallel with two MOSFETs, which are connected in back-to-back configuration. The full-wave SCC circuit is then connected in series with the resonant capacitor C_s , forming the equivalent resonant capacitor. Fig. 4 presents the operation waveform of the circuit.

The operation principle of the full-wave SCC circuit can be summarized as follows. Assuming a sinusoidal current I_{AB} is flowing through the circuit, the current zero-crossing points are at angle $0, \pi, 2\pi, \dots$ etc. For a positive half cycle, SCC1 is turned off at angle $2n\pi+\alpha$, or α degree after the zero-crossing points (from negative to positive) of the current. After SCC1 is turned off, current I_{AB} flows from

A to B via the capacitor C_a . Due to the large capacitance of C_a , the voltage V_{Ca} increases slowly, leading to ZVS turn-off for SCC1. The current keeps charging the capacitor C_a until next current zero-crossing point at $(2n+1)\pi$. Then, the current I_{AB} reverses direction, and begins to discharge the capacitor C_a . After C_a is fully discharged, the negative current is about to flow from B to A via the body diode of SCC1. To achieve ZVS turn-on and prevent the body diode from conducting, SCC1 is turned on as soon as the capacitor voltage drops to zero. It remains on for the rest of cycle and turns off again at angle $(2n+2)\pi+\alpha$. Following the same procedure, SCC2 controls the negative half cycle. It is turned off at angle $(2n+1)\pi+\alpha$, or α degree after the zero-crossing points (from positive to negative) of the current. When capacitor voltage V_{Ca} discharges to zero, SCC2 is

turned on with ZVS. Besides, due to the large capacitance of C_a , ZVS turn-off can also be achieved for SCC2.

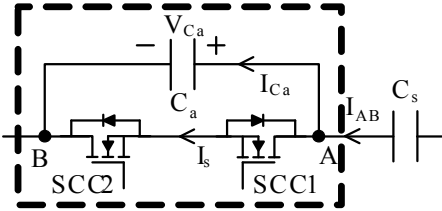


Fig. 3. Structure of a full-wave SCC circuit

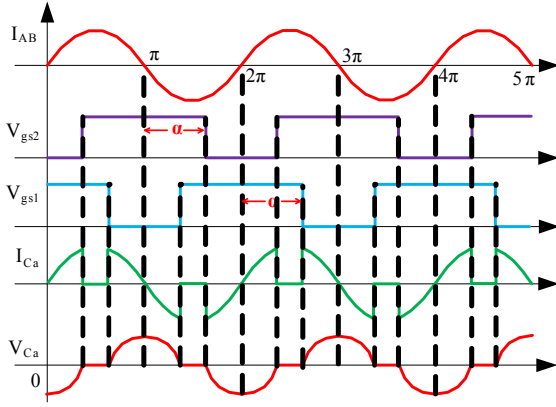


Fig. 4. Operation waveform of a full-wave SCC circuit

Only SCC1 and SCC2 are turned on at the same time, the current I_{AB} will flow through the SCC MOSFETs; otherwise, it will flow via the capacitor C_a to charge and discharge it. Considering the fundamental components in V_{Ca} and I_{AB} fourier series, the equivalent capacitance of full-wave SCC circuit, C_{SC} can be calculated as a function of delay angle α ,

$$C_{SC} = \frac{C_a}{2 - (2\alpha - \sin(2\alpha))/\pi} \quad (1)$$

The equivalent resonant capacitance equals to the series connection of the C_{SC} and the C_s . It can then be derived as,

$$C_r = \frac{\pi C_a C_s}{\pi C_a + 2\pi C_s - 2\alpha C_s + \sin(2\alpha) C_s} \quad (2)$$

When α equals to 90° , there is no overlapping turn-on between SCC1 and SCC2. Current I_{AB} always flows through the capacitor C_a , making it fully connected into the resonant tank. The equivalent resonant capacitance is at the minimum value which is equal to C_s and C_a connected in series. On the other hand, when α increases to 180° , SCC1 and SCC2 are always turned on, and the capacitor C_a is short circuit by two MOSFETs. The equivalent resonant capacitance is at its maximum value C_s . Fig. 5 shows the ratio of equivalent resonant capacitor C_r over series resonant capacitor C_s with respect to SCC angle α . In this example, C_s is 3.4nF , and C_a is 10nF . From Fig. 5, the equivalent resonant capacitor is between $0.75 \times 3.4\text{nF}$ and $1 \times 3.4\text{nF}$. By controlling angle α , the equivalent resonant capacitance can be modified.

Besides the SCC circuit could only reduce the equivalent resonant capacitance through decreasing its angle α .

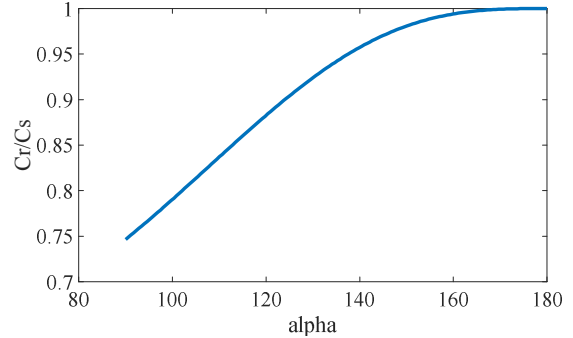


Fig. 5. Capacitance ratio of C_r over C_s with respect angle α

III. LOAD SHARING CHARACTERISTIC OF LLC CONVERTER

Based on time-domain analysis, the voltage gain of full bridge LLC converter in boost mode can be derived as [7, 8],

$$\frac{V_o}{V_{in}} = -\frac{2}{n} \frac{Z_o \omega_o}{4n^2 f_{sw} R} (\cos\beta - 1) + \frac{1}{2L_m \omega_o} \sin\beta - (\cos\beta + 1) \quad (3)$$

Where, all definitions are given as,

$$Z_o = \sqrt{\frac{L_r}{C_r}}, \quad Z_1 = \sqrt{\frac{L_r + L_m}{C_r}}, \quad \omega_o = \frac{1}{\sqrt{L_r C_r}}, \quad \omega_l = \frac{1}{\sqrt{(L_r + L_m) C_r}}, \\ \beta = \pi \omega_l \left(\frac{1}{2\pi f_{sw}} - \frac{1}{\omega_o} \right) \quad (4)$$

The output current can then be calculated as,

$$I_o = \frac{4n^2 f_{sw} V_o}{Z_o \omega_o (\cos\beta - 1)} \left(\cos\beta + 1 - \frac{2V_{in}}{nV_o} - \frac{\pi Z_1}{2L_m \omega_o} \sin\beta \right) \quad (5)$$

Where, ω_s is switching frequency in radians. ω_o is resonant frequency in radians.

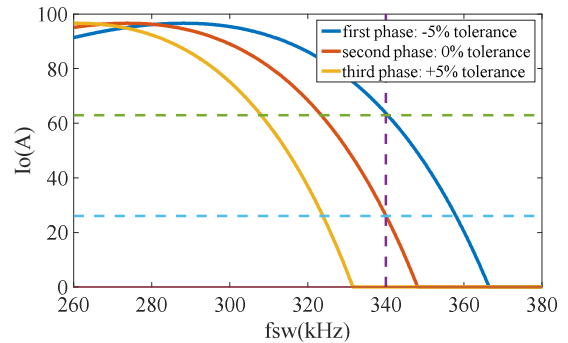


Fig. 6. Output current of LLC converter at 380V input 14V output

Fig. 6 shows the output current versus switching frequency at 380V input, 14V output. The nominal values of resonant tank components L_r , L_m , and C_r are $25\mu\text{H}$, $125\mu\text{H}$, and 3.4nF , respectively. For the first phase, -5% tolerance is assumed on L_r , L_m , and C_r . For the second phase and the third phase, 0% and $+5\%$ tolerances are assumed on L_r , L_m ,

and C_r . Taking 340kHz frequency as an example, the output current for three phases are 63A, 26A and 0A, confirming that there is no current sharing among three phases if component tolerance is considered.

To compensate component tolerance and achieve load sharing, full-wave SCC circuit is applied into the resonant tank. By controlling the delay angle α , the equivalent resonant capacitor C_r is adjusted so that the voltage gain could be modified to match with each other at same switching frequency. Thus, current sharing could be obtained. With SCC compensation, the output current of LLC converter can be recalculated as,

$$I_o(f_{sw}, \alpha) = \frac{4n^2 f_{sw} C_r(\alpha) V_o}{\cos \beta - 1} \left(\cos \beta + 1 - \frac{2V_{in}}{nV_o} - \frac{\pi}{2} \sqrt{\frac{1}{L_m} \left(\frac{1}{L_r} + \frac{1}{L_m} \right)} \sin \beta \right) \quad (6)$$

Where, $C_r(\alpha)$ is a function of delay angle α , defined in (2).

Defining the actual values of resonant components for three phases are L_{r1} , L_{m1} , C_{s1} , C_{a1} , L_{r2} , L_{m2} , C_{s2} , C_{a2} , and L_{r3} , L_{m3} , C_{s3} , C_{a3} , respectively. Tolerances on resonant components are included. With a good SCC compensation, the output currents of three phases will be the same. Thus, the following relationship can be built,

$$\begin{cases} I_{o1}(f_{sw}, \alpha_1) = I_{o2}(f_{sw}, \alpha_2) \\ I_{o2}(f_{sw}, \alpha_2) = I_{o3}(f_{sw}, \alpha_3) \\ I_{o3}(f_{sw}, \alpha_3) = I_{o1}(f_{sw}, \alpha_1) \end{cases} \quad (7)$$

There are four unknown parameters in three equations, which are switching frequency f_{sw} , and delay angle α_1 , α_2 , and α_3 . In theory, multiple combinations of f_{sw} and delay angle α can be derived to meet current sharing requirement. To solve (7), either f_{sw} or one of the delay angle α should be assigned to a given value. Compared to f_{sw} , α is designed to offset resonant component tolerance, which will have trivial impact on the normal operation of the LLC converter. Therefore, it is reasonable to set one of the α to a given value from 90° to 180° . However, large given value provides several advantages over small given value. Specifically,

- 1) Lower voltage rating on SCC MOSFETs. The voltage rating of SCC MOSFET is the maximum voltage across SCC capacitor C_a , and it can be calculated as,

$$V_{Ca_max} = \frac{1}{C_a} \int_0^{(\pi-\alpha)T_{sw}} i_{AB}(t) dt \quad (8)$$

Where, $i_{AB}(t)$ is the current flowing through SCC circuit. Larger angle α leads to shorter charging time for C_a , and lower voltage across it. Thus, lower voltage rating MOSFETs can be used which usually have low turn-on resistance.

- 2) Less deviation on quality factor. The quality factor of the LLC converter is derived as,

$$Q = \frac{\pi^2 I_o \sqrt{L_r / C_r}}{8n^2 V_o} \quad (9)$$

The modified quality factor will be equal to the nominal quality factor, if angle α approaches to 180° . Therefore, the LLC operation points with SCC compensation will be closer to the pre-designed operation points with nominal resonant parameters, which usually have been optimized.

- 3) Larger tolerance compensation margin. SCC circuit offsets component tolerance by reducing angle α . For full-wave SCC, it will loss compensation capacity when angle α is decreased to 90° . Therefore, large angle α provides more compensation margin than small angle α .

To verify the correctness of the analysis, the following two simulation cases are studied and compared.

Case 1: $\alpha_1 = 180^\circ$

As shown in Fig. 6, the phase with -5% tolerance outputs 63A load at 380V input 14V output, 340kHz frequency. To achieve current sharing, the other two phases should provide same amount of load current. Thus, the total output current will be 190A. Fig. 7 shows the simulation result of secondary side rectified current at 380V input, 14V/190A output, and 340kHz frequency without SCC compensation. From Fig. 7, the average rectified current of three phases are 144A, 46A and 0A, respectively. The resonant component tolerance causes severe current unbalance.

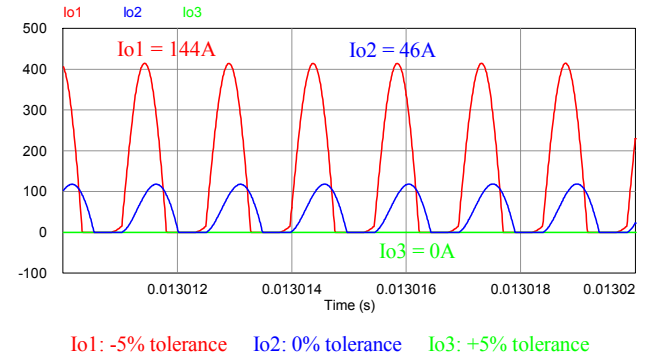
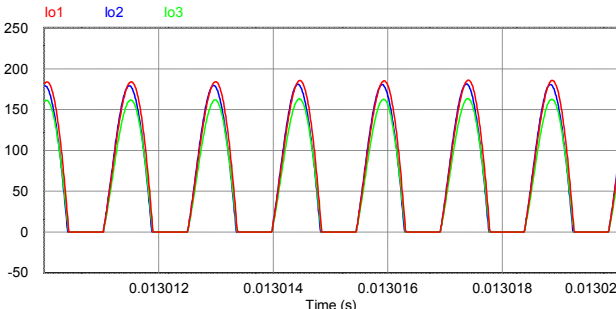


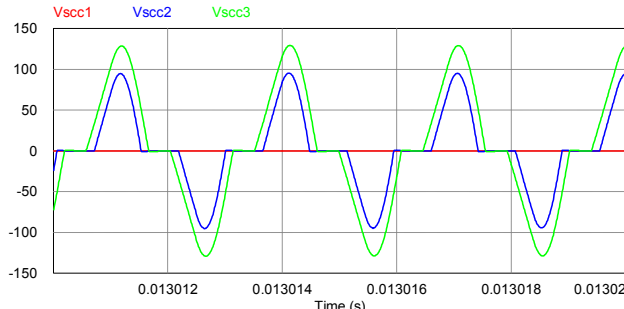
Fig. 7. Secondary side rectified current at 380V input, 14V output and 340kHz frequency without SCC compensation

Fig. 8 also shows the simulation result of the secondary side rectified current and the SCC capacitor voltage at 380V input, 14V/190A output, and 340kHz frequency. SCC compensation is applied in this simulation case. Angle α_1 of the -5% tolerance phase is set to 180° ; angle α_2 of the 0% tolerance phase is set to 123° ; and angle α_3 of the +5% tolerance phase is set to 103° . From Fig. 8(a), three phases carry almost the same amount of load. The average value of the rectified current is around 63A. Current sharing is obtained by using SCC circuit. The capacitor voltage of the -5% tolerance phase is zero, as the capacitor is short circuit by SCC MOSFETs. In addition, the peak capacitor voltage of the +5% tolerance phase is 130V.



Io1: -5% tolerance Io2: 0% tolerance Io3: +5% tolerance

(a) Secondary side rectified current



Vscc1: -5% tolerance Vscc2: 0% tolerance Vscc3: +5% tolerance
(b) SCC capacitor voltage

Fig. 8. Secondary side rectified current and SCC capacitor voltage at 380V input, 14V output and 340kHz frequency with SCC compensation

Case 2: $\alpha_1 = 150^\circ$

If set angle α_1 of the -5% tolerance phase to 150° , another combination of α_2 , α_3 , and f_{sw} could be solved. To output 63A load at 380V input and 14V output, the switching frequency of the -5% tolerance phase is increased to 343kHz. The required α_2 and α_3 of 0% and +5% tolerance phases should be set to 118° and 99° .

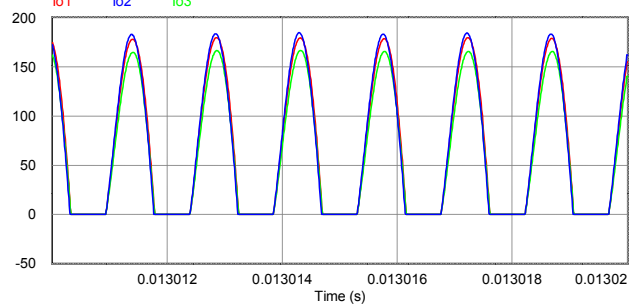
Fig. 9 shows the simulation result of the secondary side rectified current and the SCC capacitor voltage at 380V input, 14V output, and 343kHz frequency. The SCC angle α for three phases are set to 150° , 118° , and 99° , respectively. Good current sharing performance is also achieved. However, the peak capacitor voltage of the +5% tolerance phase is increased to 145V.

Simulation results verified that multiple combinations of f_{sw} and angle α are existing to satisfy current sharing requirement. The decreasing on angle α_1 results in the decreasing on α_2 and α_3 , and the increasing on SCC capacitor peak voltage. Moreover, the solution with larger angle α could help reduce the voltage rating for SCC MOSFETs.

IV. SCC CONTROL STRATEGY

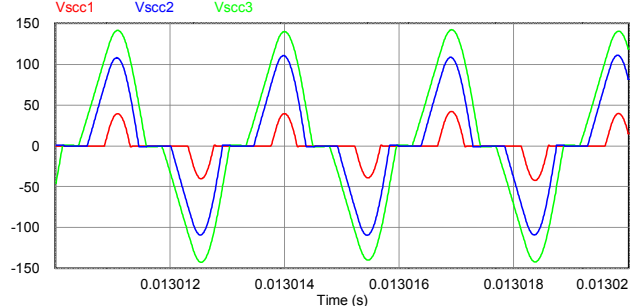
In this work, two Microchip DSCs dsPIC33FJ32GS610 are used to implement the proposed control scheme. One MCU is in the LLC converter primary side and the other one is placed in the secondary side.

The voltage loop is implemented in secondary side MCU by using conventional PI control method. Frequency modulation is used to regulate the output voltage to its desired value. The digital implementation of the voltage loop is shown in Fig. 10. An isolated gate driver is used to transfer the PWM signal generated by the MCU from secondary side to primary side switches.



Io1: -5% tolerance Io2: 0% tolerance Io3: +5% tolerance

(a) Secondary side rectified current



Vscc1: -5% tolerance Vscc2: 0% tolerance Vscc3: +5% tolerance

(b) SCC capacitor voltage

Fig. 9. Secondary side rectified current and SCC capacitor voltage at 380V input, 14V output and 343kHz frequency with SCC compensation

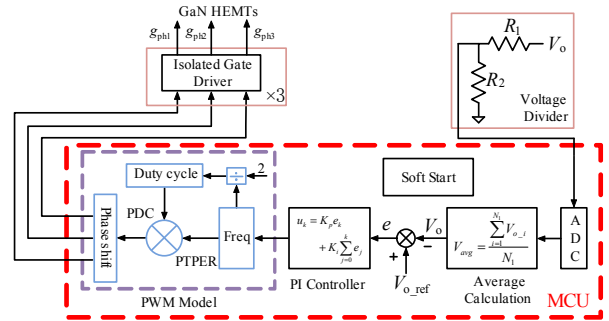


Fig. 10. Digital implementation of voltage loop

The current loop is implemented in primary side MCU. Three phases' input current are sensed and compared to estimate the output current sharing. To avoid oscillation, the current loop is designed much slower than that of the voltage loop. The control process of the current loop is described as follows.

At the beginning, all three phases SCC angle α are set to the maximum value. The average values of three-phase input current are sampled and compared in MCU. Of all three phases, there is one phase which provides the highest current; and there is another phase which carries the lowest current. Based on comparison result, firstly, the SCC angle α of the highest current phase will be increased by $\Delta\alpha$ degree to decrease its output current. If the angle α of the highest current phase equals to its maximum value, then, the SCC angle α of the smallest current phase starts to decrease by $\Delta\alpha$ degree to increase its output current. After n comparison cycles, the angle α will be increased and/or decreased by $\Delta\alpha \times n$. The difference among three-phase currents will become smaller, and finally, the total output current will be distributed into three phases equally. The proposed controller always increases the angle α of the highest current phase at first, then decreases the angle α of the lowest current phase so that current sharing can be achieved with large angle α . The digital implantation of the proposed current loop is shown in Fig. 11.

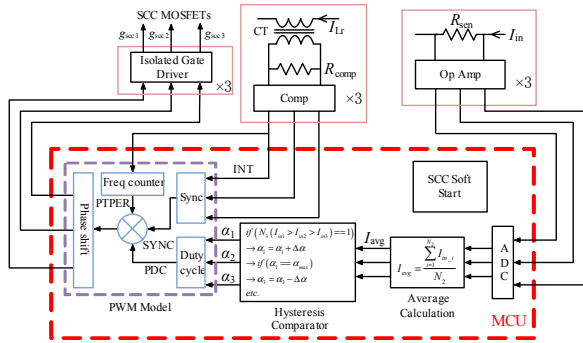


Fig. 11. Digital implementation of the proposed current loop

PWM module is used to generate gate single for SCC MOSFETs. The PWM signal is synchronized with the zero-crossing points of resonant current of corresponding phase. A current transformer (CT) and a comparator are applied to detect the resonant current zero-crossing point. Then, the output of the comparator is transmitted to MCU as an external interrupt (INT) to reset SCC PWM signal every switching cycle.

In theory, the PWM signal is set to high when the SCC capacitor voltage drops to zero. Thus, the SCC capacitor voltage needs to be sensed and extra sensing circuit are needed. Considering the fact that the series resonant currents at both side of the zero-crossing point are almost symmetric for LLC converter, the PWM signal is set to high at angle $2n\pi - \alpha$ in practice. It is set to low still at $2n\pi + \alpha$. Therefore, the SCC capacitor has the same charging and discharging time. ZVS turn-on can still be guaranteed. No extra sensing circuit is needed.

V. EXPERIMENTAL RESULTS

To verify the effectiveness of the designed three-phase SCC-LLC converter and the proposed SCC control strategy, a 250V – 430V input, 14V/260A output prototype was built

and tested, as shown in Fig. 12. The test bench is shown in Fig. 13. The parameters of the developed prototype are shown in Table I. The maximum delay angle α is set to 140° in the testing.

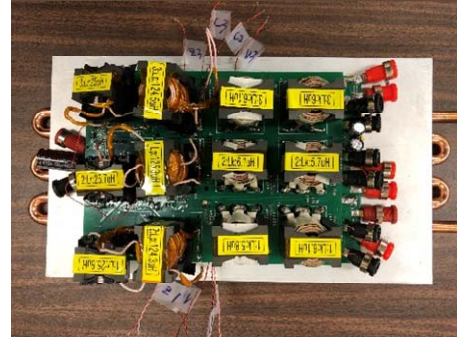


Fig. 12. Prototype of the designed three-phase SCC-LLC resonant converter



Fig. 13. Test bench of the designed three-phase SCC-LLC resonant converter

TABLE I. PARAMETERS OF THREE-PHASE SCC-LLC CONVERTER

Transformer	$N = 44$, PQ35/35 core
Parallel inductor	$L_{m1} = 125.5\mu\text{H}$, $L_{m2} = 124.2\mu\text{H}$, $L_{m3} = 127.2\mu\text{H}$, PQ35/35 core
Series inductor	$L_{r1} = 26.1\mu\text{H}$, $L_{r2} = 25.7\mu\text{H}$, $L_{r3} = 26.1\mu\text{H}$, PQ32/20 core
Series capacitor	C1808C681JGGAC7800 2KV, 680pF $\times 5$ (per phase)
SCC capacitor	C2012NP02W472J125AA, 450V, 4700pF $\times 3$ (per phase)
Primary side GaNs	GS66508B (650V, 30A) $\times 4$ (per phase)
Secondary side SRs	TPHR8504PL (40V, 150A) $\times 12$ (per phase)
SCC MOSFETs	IPB200N25N3 (250V, 64A) $\times 2$ (per phase)
Output capacitor	C3216JB1E336M160AC, 25V, 33 μF $\times 10$ (per phase)
MCU	DSPIC33FJ32GS610 $\times 2$

Fig. 14 shows the waveforms of single-phase SCC-LLC resonant converter at 380V input, 14V/90A output. The angle α is set to 140°. From Fig. 14, both SCC MOSFETs are turned on as soon as the capacitor voltage is discharged to zero to achieve ZVS operation. Moreover, the SCC capacitor voltage increases slowly after MOSFET is turned off. Thus, ZVS turn-off can also be obtained. The

body diodes of the SCC MOSFETs do not conduct. Fig. 15 compares the measured efficiencies of single-phase converter with and without SCC at 380V input. When output current is below 55A, the efficiency with SCC circuit is lower than that of without SCC circuit. However, it becomes higher at heavy load condition. Thanks to the ZVS turn-on and turn-off, SCC circuit does not have much impact on efficiency.

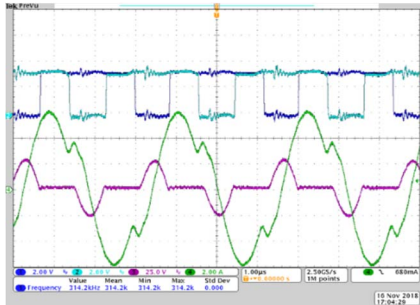


Fig. 14. Waveform of single-phase SCC-LLC converter at 380V input, 14V/90A output

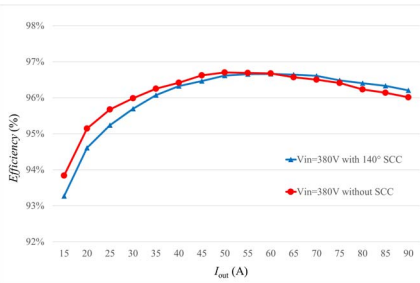


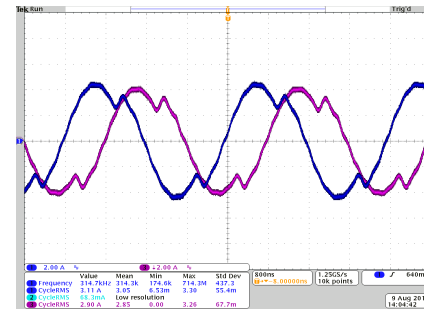
Fig. 15. Measured efficiency of single-phase LLC converter with and without SCC circuit at 380V input, 14V output

To improve the light load efficiency, phase shedding technique is performed. The prototype is tested with single-phase, two-phase and three-phase operations, respectively. Taking 380V input, 14V output as an example, the converter operates at single-phase model if output current is less than 70A. However, if output current is between 70A and 140V, the converter operates at two-phase model. In addition, if the output current is above 140A, the converter operates at three-phase model.

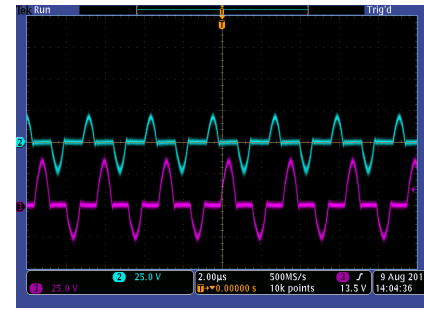
Fig. 16 shows the waveforms of the resonant current and the SCC capacitor voltage with two-phase operation at 380V input, 14A/130A output. 90° phase shift is implemented to attenuate the output voltage ripple. The first phase and the third phase are enabled. The second phase is shut down. From Fig. 16, the primary side RMS currents for both two phases are 3.11A, and 2.90A. Good current sharing between two phases is achieved. Moreover, the first phase angle α is at its maximum value, 140°.

Fig. 17 shows the waveforms of the resonant current and the SCC capacitor voltage of three-phase SCC-LLC converter at 380V input, 14A/260A output with 0°, 60° and 120° interleaving. It can be observed from Fig. 17 that the current sharing among three phases is also obtained. The primary side RMS currents of three phases are 3.86A, 3.93A

and 4A, respectively. The peak voltage of SCC capacitor for the third phase is 75V at the testing condition. The second phase angle α is at 140°.

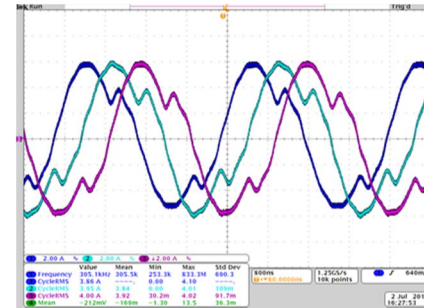


(a) series resonant current

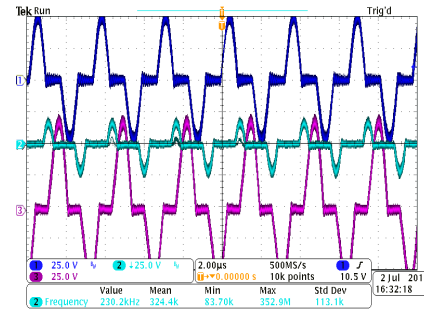


(b) SCC capacitor voltage

Fig. 16. Waveform of resonant current and SCC capacitor voltage with two-phase operation at 380V input, 14V/130A output



(a) series resonant current



(b) SCC capacitor voltage

Fig. 17. Waveform of resonant current and SCC capacitor voltage with two-phase operation at 380V input, 14V/260A output

The output side of all three phases are connected in parallel. Thus, it is difficult to measure the output current

carried by each phase directly. The RMS value of series resonant current is used to investigate the current sharing performance. Fig. 6.18 shows the RMS value of series resonant current from 70A to 130A load at 380V input, 14V output with two-phase operation. Fig. 6.19 shows the RMS value of series resonant current from 140A up to 260A load at 380V input, 14V output with three-phase operation. The RMS current difference is around 0.2A with two-phase operation. However, with three-phase operation, the difference is reduced to around 0.1A. With three-phase operation, the current sharing performance is better.

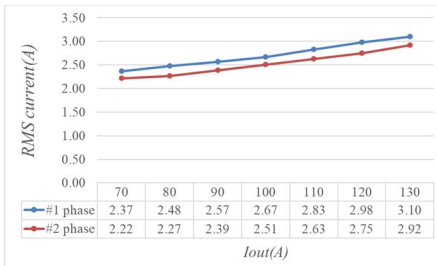


Fig. 18. RMS value of series resonant current at 380V input with two-phase operation

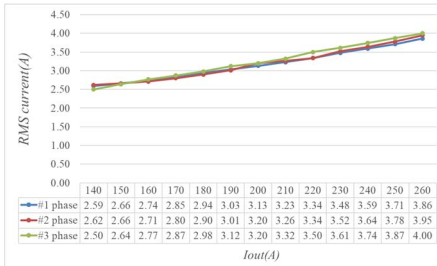


Fig. 19. RMS value of series resonant current at 380V input with three-phase operation

Fig. 20 shows the overall efficiency from light load to heavy load at 380V input. It can be observed from Fig. 20, the efficiency curve is quite stable when output current is above 40A. Thanks to phase shedding technique, the efficiency at light load has been improved. The minimum efficiency is above 91%. In addition, a peak efficiency of 96.4% and a full load efficiency of 95.7% are obtained.

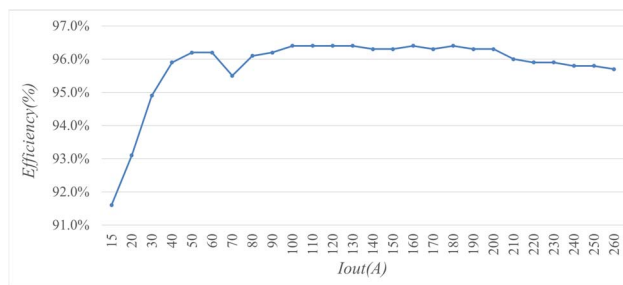


Fig. 20. Measured efficiencies at 380V input, 14V output with phase shedding

VI. CONCLUSION

Three-phase interleaved LLC converter is designed for high power EV HV to LV DC/DC converter application. Full-wave SCC circuit is applied into the converter to compensate the resonant tank component tolerance and achieve current sharing. Due to the ZVS turn-on and turn-off, the SCC circuit does not have much impact on the efficiency. The load sharing characteristic of LLC converter with and without SCC is analyzed and compared. A digital comparison control strategy is proposed to control SCC circuit for current sharing, while reducing the voltage rating for SCC MOSFETs. Phase shedding technique is used to improve light load efficiency. Experimental results of a 250V – 430V input, 14V/260A output, three-phase interleaved SCC-LLC prototype demonstrate the effectiveness of the SCC circuit and the correctness of the control strategy. Good current sharing performance and high efficiency are obtained at the same time.

REFERENCES

- [1] R. Hou and A. Emadi, "Applied Integrated Active Filter Auxiliary Power Module for Electrified Vehicles With Single-Phase Onboard Chargers," *IEEE Transactions on Power Electronics*, vol. 32, no. 3, pp. 1860-1871, 2017.
- [2] B. Kim, K. Park, C. Kim, B. Lee, and G. Moon, "LLC Resonant Converter With Adaptive Link-Voltage Variation for a High-Power-Density Adapter," *IEEE Transactions on Power Electronics*, vol. 25, no. 9, pp. 2248-2252, 2010.
- [3] D. İ and B. Erkmen, "A Very Low-Profile Dual Output LLC Resonant Converter for LCD/LED TV Applications," *IEEE Transactions on Power Electronics*, vol. 29, no. 7, pp. 3514-3524, 2014.
- [4] G. Wen-Jian and K. Harada, "A new method to regulate resonant converters," *IEEE Transactions on Power Electronics*, vol. 3, no. 4, pp. 430-439, 1988.
- [5] Z. Hu, Y. Qiu, Y. Liu, and P. C. Sen, "A Control Strategy and Design Method for Interleaved LLC Converters Operating at Variable Switching Frequency," *IEEE Transactions on Power Electronics*, vol. 29, no. 8, pp. 4426-4437, 2014.
- [6] Z. Hu, Y. Qiu, L. Wang, and Y. Liu, "An Interleaved LLC Resonant Converter Operating at Constant Switching Frequency," *IEEE Transactions on Power Electronics*, vol. 29, no. 6, pp. 2931-2943, 2014.
- [7] T. Liu, Z. Zhou, A. Xiong, J. Zeng, and J. Ying, "A Novel Precise Design Method for LLC Series Resonant Converter," in *INTELEC 06 - Twenty-Eighth International Telecommunications Energy Conference*, 2006, pp. 1-6.
- [8] N. Shafei, M. A. Saket, and M. Ordonez, "Time domain analysis of LLC resonant converters in the boost mode for battery charger applications," in *2017 IEEE Energy Conversion Congress and Exposition (ECCE)*, 2017, pp. 4157-4162.